Journal of ELECTRONIC MATERIALS, Vol. 30, No. 9, 2001 *Special Issue Paper*

Studies of the Ag-In Phase Diagram and Surface Tension Measurements

Z. MOSER,[1] W. GASIOR,[1] J. PSTRUS,[1] W. ZAKULSKI,[1] I. OHNUMA,[2] X.J. LIU,[2] Y. INOHANA,[2] and K. ISHIDA[2]

1.—Polish Academy of Sciences, Institute of Metallurgy and Materials Science, 30-059 Kraków, Reymonta Street 25, Poland. 2.—Tohoku University, Department of Materials Science, Aramaki Aoba-yama 02, Sendai 980-8579, Japan

The phase boundaries of the Ag-In binary system were determined by the diffusion couple method, differential scanning calorimetry (DSC) and metallographic techniques. The results show that the region of the ζ (hcp) phase is narrower than that reported previously. Thermodynamic calculation of the Ag-In system is presented by taking into account the experimental results obtained by the present and previous works, including the data on the phase equilibria and thermochemical properties. The Gibbs energies of liquid and solid solution phases are described on the basis of the sub-regular solution model, and that of the intermetallic compounds are based on the two-sublattices model. A consistent set of thermodynamic parameters has been optimized for describing the Gibbs energy of each phase, which leads to a good fit between calculated and experimental results. The maximum bubble pressure method has been used to measure the surface tension and densities of liquid In, Ag, and five binary alloys in the temperature range from 227°C to about 1170°C. On the basis of the thermodynamic parameters of the liquid phase obtained by the present optimization, the surface tensions are calculated using Butler's model. It is shown that the calculated values of the surface tensions are in fair agreement with the experimental data.

Key words: Phase diagram, thermodynamic calculation, surface tension, Pb-free solder

INTRODUCTION

In view of the increasing concerns over the health hazards associated with the presence of lead in the environment, very substantial efforts are being made to eliminate lead-base solders. The Ag-In system is one of the basic systems for the development of the Pb-free micro-solder alloys. The phase diagram of the Ag-In system was assessed by Baren,[1] as shown in Fig. 1. The intermediate phases—ζ (hcp), γ ($D8_3$:Ag_2In), β (A2), and φ (C16:$AgIn_2$)—were identified by Weibke,[2] Hellner,[3] Frevel and Ott,[4] as well as by Campbell.[5] However, very few data on the phase boundaries and the reactions involving ζ phase have been reported.

The thermodynamic properties of this system were also investigated by Kleppa,[6] Orr and Hultgren,[7] Nozaki,[8] Beja,[9] Alcock,[10] Castanet,[11] Predel and Schallner,[12] Masson,[13] Alcock,[14] Kameda,[15] Qi,[16] and Bienzle and Sommer.[17] A thermodynamic assessment of this system was carried out by Kornenhen and Kivilahti;[18] however, a good agreement was not obtained between calculated and experimental results with regard to the phase equilibria associated with ζ phase.

The surface tension, which is one of the critical physical properties of solder, is important for the development of solder alloys. Detailed investigations on the surface tension of the liquid phase in the Ag-In system were not found.

The purpose of the present study is (1) to determine the phase equilibria on the basis of the diffusion couple method, differential scanning calorimetry

(Received February 13, 2001; accepted April 17, 2001)

(DSC), and metallography; (2) to assess thermodynamically the phase diagram of the Ag-In system based on the experimental data; (3) to perform the measurements of the surface tension and densities of the liquid phase by the maximum bubble pressure method; and (4) to predict the surface tension of the liquid phase using the optimized thermodynamic parameters with the aid of Butler's method.[19]

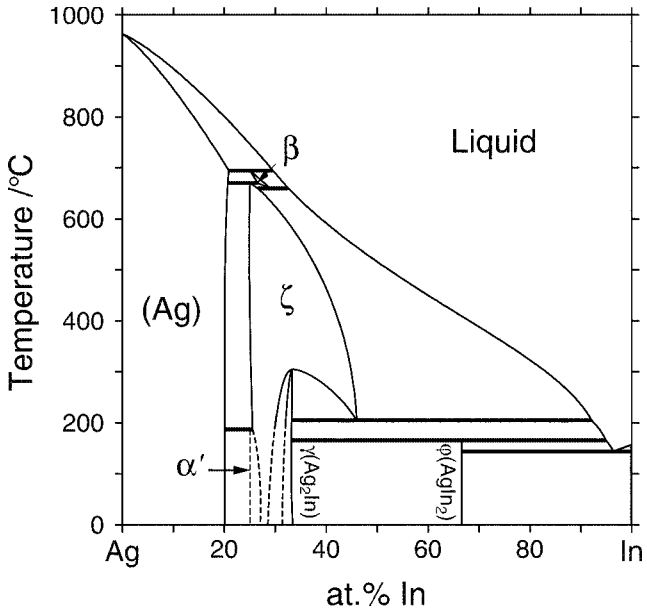

Fig. 1. Phase diagram of the Ag-In binary system.[1]

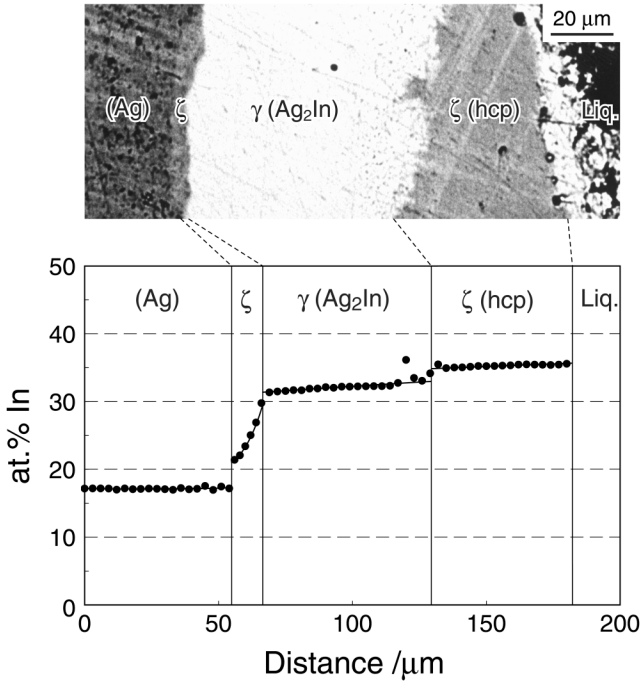

Fig. 2. Microstructure and concentration profile of the Ag-15at.%In/In diffusion couple annealed at 250°C for 216 h.

EXPERIMENTAL PROCEDURE

Determination of Phase Equilibria

Binary Ag-In alloys were prepared using pure Ag (99.99%) and In (99.99%) by melting under an argon atmosphere. All alloys were homogenized at different temperatures from 180°C to 600°C and then quenched. The microstructures of specimens were examined by optical microscopy after heat treatment. A (H_2O:28%NH_3:H_2O_2=1:1:1) solution was used as the etchant for metallographic examination. The equilibrium compositions were determined by electron probe microanalysis (EPMA) using specimens with two-phase structures. A solid/liquid diffusion couple Ag-15at.%In / In was also used to determine the phase equilibria at different temperatures in a wide range of composition. The methods of preparation of diffusion couples and of examination of the phase equilibria

Table 1 Equilibrium compositions determined by present work.

Phase equilibria	Temperature [°C]	Equilibrium composition [at.% In]		Remarks
phase1 / phase2		phase1	phase2	
(Ag) / ζ	600	19.7	23.2	T.S.
	500	19.4	22.4	T.S.
	400	19.1	22.4	T.S.
	250	18.7	22.4	T.S.
	250	17.9	22.1	T.S.
ζ / Ag_2In	250	30.1	31.3	T.S.
	250	30.5	32.2	T.S.
	250	36.2	33.8	D.C.
Ag_2In / liquid	180	33.1	67.0	D.C.
ζ / liquid	500	33.5	-	T.S.
	400	34.7	-	T.S.
	300	35.0	-	T.S.
	250	35.1	-	T.S.
	250	37.2	-	D.C.

T.S.: Two-phase specimen. D.C.: Diffusion couple.

Table 2 Temperatures of phase transformation determined by DSC.

at.% In	Temperature of phase transformation [°C]	
	Liquidus	Other transformation
10	907	863
15	867	788
22.5	791	184, 669, 692
25	767	101, 194, 661, 673, 692
27.5	730	142, 194, 634, 659, 692
30	684	146, 595, 659
31	675	149, 568, 659
32	659	301, 542
33	651	292, 508
35	636	169, 196, 278
40	596	169, 195
60	455	168, 194
80	361	145, 171

were identical to those described in our previous paper.[20] The prepared diffusion couples were sealed in transparent quartz capsules and equilibrated in the temperature range from 250°C to 600°C for 1.5–20 days and then quenched into iced water. Equilibrium compositions can be obtained by extrapolating the concentration profile curves to the interface boundary. Liquidus temperatures and phase transformation temperatures were also determined by DSC experiments, which were carried out in an atmosphere of flowing argon. The samples were heated and cooled at rates of 0.5–5°C/min using sintered Al_2O_3 as the reference specimen, and the data are taken from the heating curve.

Measurements of Surface Tension and Density

The maximum bubble pressure method has been used to measure the surface tension of In, Ag, and five of their binary alloys with indium concentrations of 20, 35, 45.4, 58, and 80 at.% in the temperature range from 227°C to about 1170°C, with the range depending on the composition of the investigated alloy. This method is based on the Laplace equation describing the relation between surface tension, σ, radius of

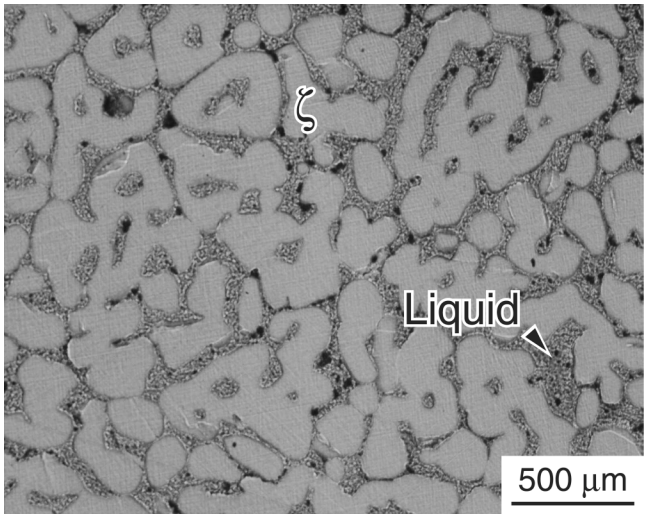

Fig. 3. Two-phase microstructure of the Ag-50at.% In alloy annealed at 300°C for 48 h.

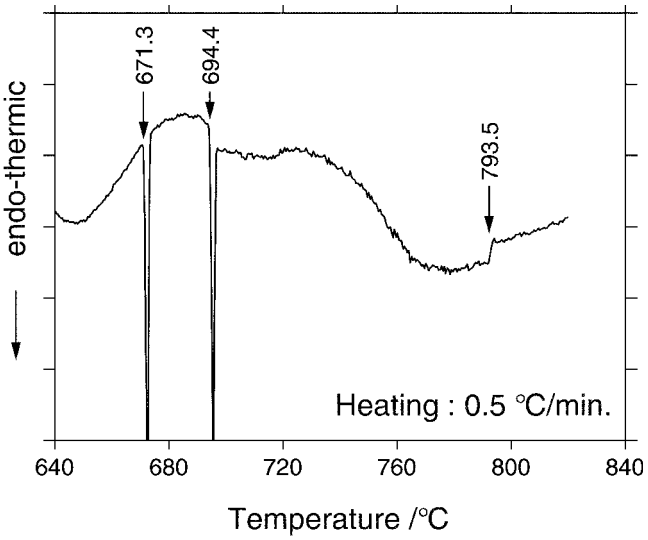

Fig. 4. DSC heating curve of the Ag-22.5 at.% In alloy.

Table 3 Thermodynamic parameters in the binary Ag-In system assessed by this work (J/mol)

Liquid	For 298.14- 1235.08 K:
	${}^{\circ}G^{liq}_{Ag}-{}^{\circ}G^{fcc}_{Ag}$ = +11025.293 -8.890146 T-1.0322×10^{-20} T^{7}
	For 1235.08- 3000.00 K:
	${}^{\circ}G^{liq}_{Ag}-{}^{\circ}G^{fcc}_{Ag}$ = +11507.972 -9.300495 T-1.412186×10^{29} T^{-9}
	For 298.14- 429.78 K:
	${}^{\circ}G^{liq}_{In}-{}^{\circ}G^{tetra}_{In}$ = +3282.152 -7.63649 T -5.21918×10^{-20} T^{7}
	For 429.78- 3800.00 K:
	${}^{\circ}G^{liq}_{In}-{}^{\circ}G^{tetra}_{In}$ = +3283.66 -7.640174 T -3.30026×10^{22} T^{-9}
	${}^{0}L^{liq}_{Ag,In}$ = -14403.297 -8.176 T
	${}^{1}L^{liq}_{Ag,In}$ = -15551.028 -2.664 T
	${}^{2}L^{liq}_{Ag,In}$ = -710.629 -5.293 T
	${}^{3}L^{liq}_{Ag,In}$ = +3955.27
(Ag) (FCC)	For 298.14- 3000.00 K:
	${}^{\circ}G^{fcc}_{In}-{}^{\circ}G^{tetra}_{In}$ = +123 -0.1988 T
	${}^{0}L^{fcc}_{Ag,In}$ = -15581.083 +10.592 T
	${}^{1}L^{fcc}_{Ag,In}$ = -31111.065 -11.376 T
ζ (HCP)	${}^{\circ}G^{hcp}_{Ag}-{}^{\circ}G^{fcc}_{Ag}$ = +300 +0.3 T
	${}^{\circ}G^{hcp}_{In}-{}^{\circ}G^{tetra}_{In}$ = 533 -0.6868 T
	${}^{0}L^{hcp}_{Ag,In}$ = -9505.055 +1.618 T
	${}^{1}L^{hcp}_{Ag,In}$ = -67897.015 +5.33 T
	${}^{2}L^{hcp}_{Ag,In}$ = +36923.27
γ (Ag_2In)	2 sublattice, site 0.68:0.32
	${}^{\circ}G^{Ag_2In}-0.68{}^{\circ}G^{fcc}_{Ag}-0.32{}^{\circ}G^{tetra}_{In}$ = -6758.7 -3.084 T
φ ($AgIn_2$)	2 sublattice, site 0.33:0.67
	${}^{\circ}G^{AgIn_2}-0.33{}^{\circ}G^{fcc}_{Ag}-0.67{}^{\circ}G^{tetra}_{In}$ = -9704.6 +12.754 T
(In) (Tetragonal)	

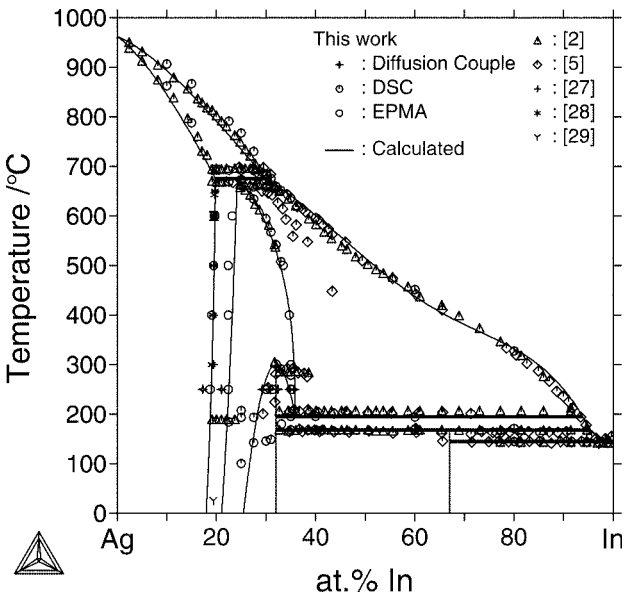

Fig. 5. Calculated phase diagram in comparison with the experimental data.

capillary, r, and the pressure required to form and to detach the gas bubble from the end of the capillary. When the capillary is immersed at the depth, h, the approximate value of the surface tension, σ, is calculated from the following equation, taking the hydrostatic pressure of liquid into account:

$$\sigma = \frac{rg}{2} \cdot (h_m \rho_m - h_c \rho_c) \quad (1)$$

where: g denotes the acceleration of gravity, h is the difference of the height of manometric fluid before and after introducing the capillary to the depth (h_c), ρ_m, and ρ_c are the densities of manometric fluid and the liquid metal ($kg \cdot m^{-3}$), respectively.

The precise values of surface tension were calculated by the Sugden's method[21] based on the tables produced by Bashforth and Adams.[22]

Densities of In and Ag were measured by dilatometric method, and those of the Ag-In alloys were calculated from the difference of the pressures measured at two depths by capillaries immersed at the same time that the measurements of the surface tensions were made.

Each alloy was separately prepared by melting metals in the protective atmosphere of high-purity

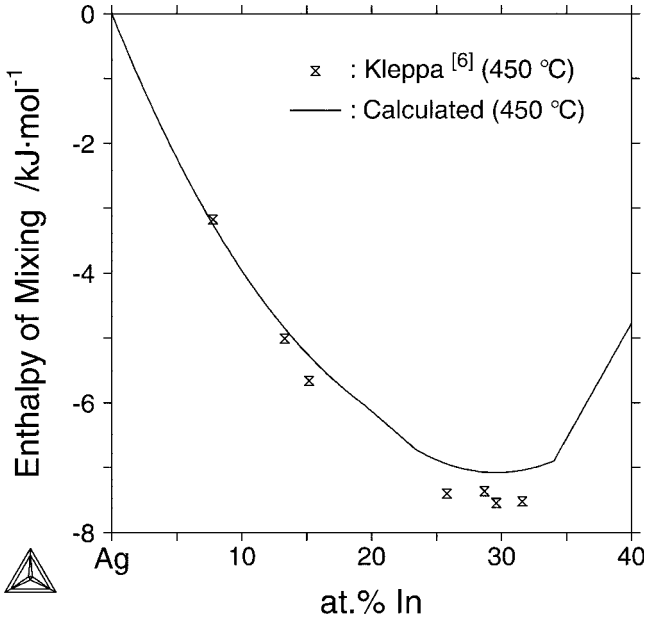

Fig. 6. Enthalpy of mixing of the solid phase in the Ag-In system.

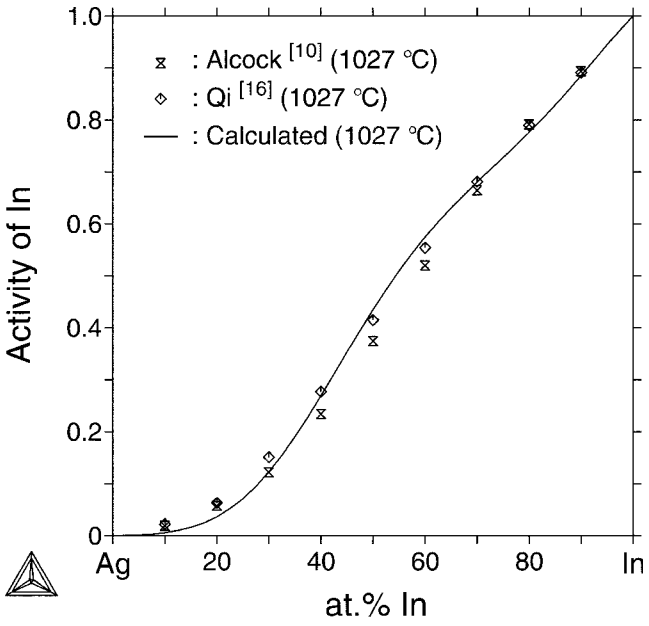

Fig. 8. Activity of In in the liquid phase in the Ag-In system.

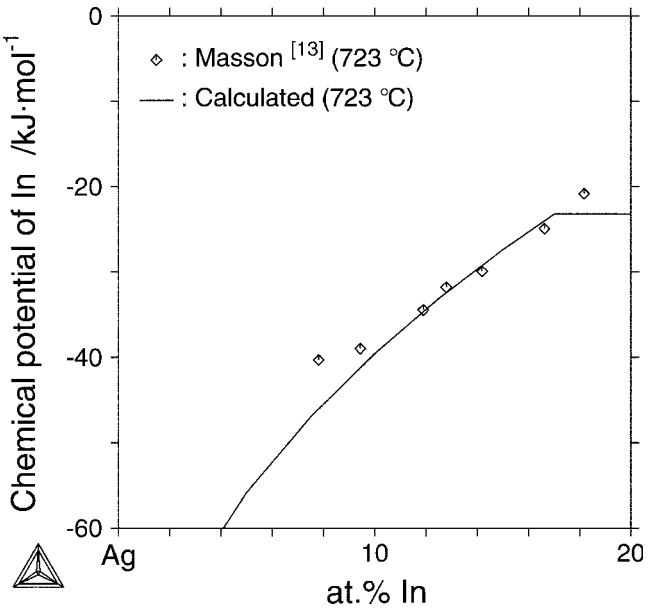

Fig. 7. Chemical potential of In in the fcc phase in the Ag-In system.

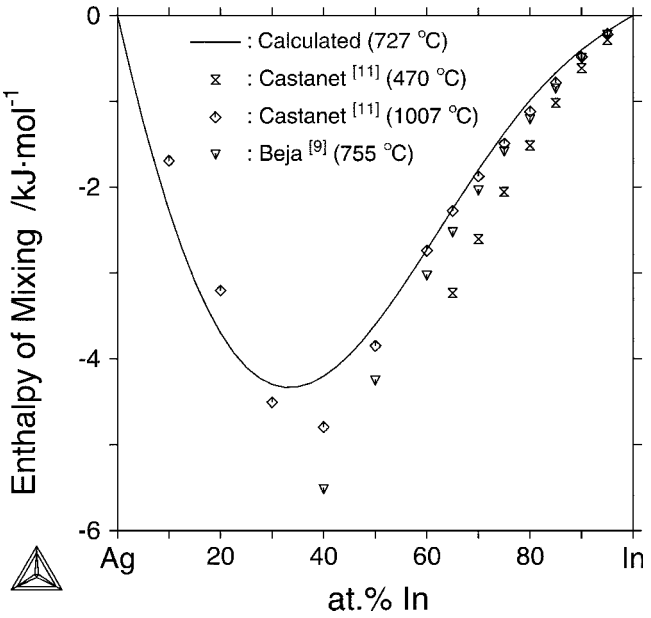

Fig. 9. Enthalpy of mixing of the liquid phase in the Ag-In system.

Ar+20 vol.% H_2 mixture. Alloys were analyzed by the atomic absorption method and used for surface tension measurements in the same protective atmosphere.

THERMODYNAMIC MODELING

Description of Gibbs Energy

Liquid and Solid Phases

The Gibbs energies of liquid ζ and Ag solid phases are described by the sub-regular solution model with the Redlich-Kister polynomial[23] as follows:

$$
\begin{aligned}
G_m^{\phi} &= {}^{o}G_{Ag}^{\phi} x_{Ag}^{\phi} + {}^{o}G_{In}^{\phi} x_{In}^{\phi} + RT(x_{Ag}^{\phi} \ln x_{Ag}^{\phi} \\
&\quad + x_{In}^{\phi} \ln x_{In}^{\phi}) + G^{E}(T, x_{In}) \\
G^{E}(T, x_{In}) &= x_{Ag}^{\phi} x_{In}^{\phi} \cdot L_{Ag,In}^{\phi} \\
L_{Ag,In}^{\phi} &= \sum_{m=0}^{n} {}^{m}L_{Ag,In}^{\phi} \cdot (x_{Ag} - x_{In})^{m}
\end{aligned}
\qquad (2)
$$

where ${}^{m}L_{Ag,In}^{\phi}$ is the temperature-dependent parameter optimized on the basis of the available thermody-

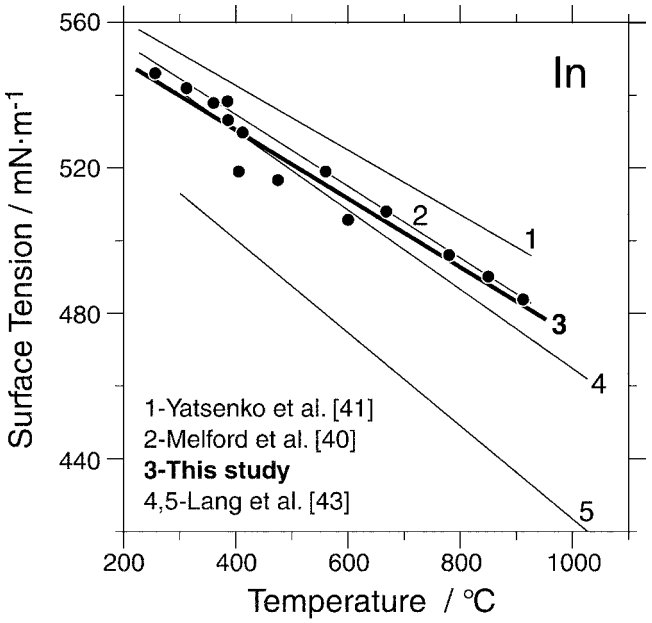

Fig. 10. Surface tension of pure In of this study (solid circles) in comparison with various references.

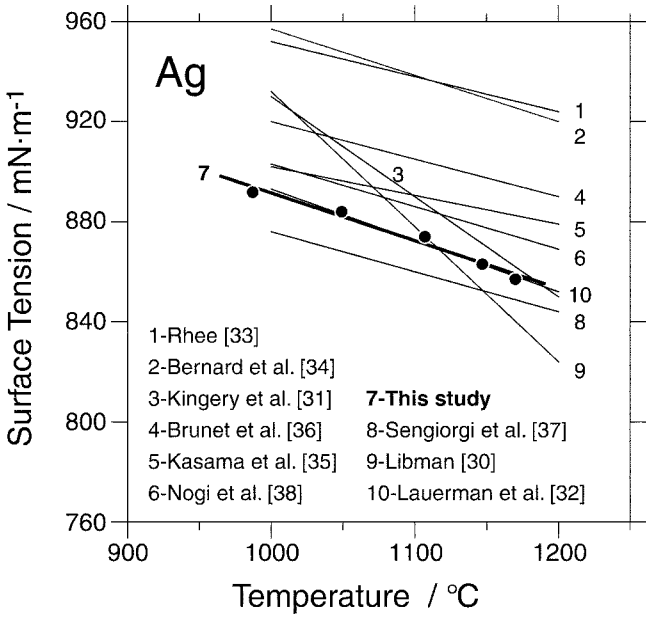

Fig. 11. Surface tension of pure Ag of this study (solid circles) in comparison with various references.

Table 4 A comparison on the invariant reactions between the present results and previous data.

Reaction	Temp. [°C]	Composition [at.% In]		
L + (Ag) ↔ β	695 [1]	Liquid	(Ag)	β
	694 (Exp.)	30.0 [1]	21.0 [1]	25.0 [1]
β + (Ag) ↔ ζ	670 [1]	β	(Ag)	ζ
	671 (Exp.)	26.5 [1]	20.9 [1]	25.0 [1]
β ↔ ζ + L	660 [1]	β	ζ	Liquid
	660 (Exp.)	30.0 [1]	28.0 [1]	32.5 [1]
L + (Ag) ↔ ζ [(a)]	675.5 (Cal.)	Liquid	(Ag)	ζ
		30.1 (Cal.)	19.8 (Cal.)	24.2 (Cal.)
ζ ↔ γ + L	195 (Cal.)	ζ	γ	Liquid
	205 [1]	35.9 (Cal.)	32.0 (Cal.)	93.9 (Cal.)
		45.9 [1]	33.5 [1]	92.2 [1]
L + γ ↔ φ	168 (Cal.)	Liquid	γ	φ
	166 [1]	95.4 (Cal.)	32.0 (Cal.)	67.0 (Cal.)
		96.2 [1]	33.5 [1]	66.7 [1]
L ↔ φ + (In)	145 (Cal.)	Liquid	φ	(In)
	144 [1]	97.6 (Cal.)	67.0 (Cal.)	100 (Cal.)
		96.8 [1]	66.7 [1]	100 [1]

(a) This reaction is metastable because the β phase was not considered in the present calculation

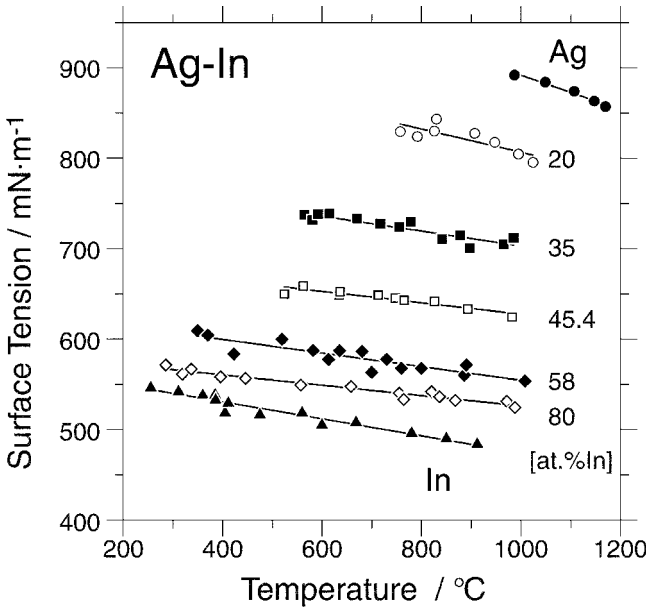

Fig. 12. Temperature dependence of the surface tensions of the liquid Ag-In alloys. Symbols: experimental data of this study. Solid lines: average from linear equations.

namic and phase diagram data. The β (bcc) phase is not considered because of the very small solubility, and the solubility of Ag in In is not taken into account in the present assessment.

Stoichiometric Compounds

The solubility of the compound phases in this system is very narrow and is not clearly determined according to the literature. In the present assessment, the γ (Ag_2In) and φ ($AgIn_2$) phases are treated as stoichiometric compounds. Then, the Gibbs energy of the compound, Ag_mIn_n, is described as

$$G_m^{Ag_mIn_n} = \frac{m}{m+n} \cdot^{o} G_{Ag}^{fcc} + \frac{n}{m+n} \cdot^{o} G_{In}^{fct} + \Delta G_{Ag_mIn_n}^{f} \quad (3)$$

where $\Delta G_{Ag_mIn_n}^{f}$ represents the Gibbs energy of formation per mole of atoms of the Ag_mIn_n compound and is expressed by the following equation:

Table 5 Temperature dependence of the surface tensions of liquid In and Ag and Ag-In alloys. Calculated from linear equations, surface tensions at 1173 K with errors and the squared coefficients of correlation.

at.% In	$\gamma = A + B \cdot T$ [mN·m^{-1}]	γ (at 1173K) [mN·m^{-1}]	Coef of determination R-squared
100	593.8 -0.094210·T	483.3 ±5.2	0.93378
80	602.0 -0.060213·T	531.4 ±6.0	0.95585
67	649.2 -0.073955·T	561.6 ±10.0	0.84543
45.4	708.2 -0.063737·T	666.5 ±7.7	0.87256
35	807.4 -0.082288·T	710.8 ±8.1	0.83795
20	962.5 -0.123334·T	817.8 ±8.5	0.87870
0	1134.0-0.190472·T	910.6 ±5.3	0.97440

Lp.	Temperature [K]	γ_{Ag} [mN·m^{-1}]	$\Delta\gamma_{Ag}$ [mN·m^{-1}]
1	1260	891.8	±5.6
2	1322	884	±5.0
3	1380	874	±5.1
4	1420	863	±5.5
5	1443	857	±5.6

$\Delta\gamma$: Cantor-Schrodinger formula

Table 6 Temperature dependence of the densities of liquid In and Ag and Ag-In alloys. Calculated from linear equations, densities at 1173 K with errors and the squared coefficients of correlation.

at.% In	$d = A + B \cdot T$ [g·cm^{-3}]	d (at 1173K) [g·cm^{-3}]	Coef. of determination R-squared
100	7.314 -0.0006842·T	6.511 ±0.036	0.9962
80	8.364 -0.0013340·T	6.799 ±0.196	0.8214
65	8.964 -0.0016271·T	7.055 ±0.135	0.8906
45.4	9.701 -0.0015789·T	7.849 ±0.189	0.7616
35	10.657 -0.0018527·T	8.484 ±0.088	0.9430
20	11.182 -0.0019249·T	8.924 ±0.079	0.8836
0	10.472 -0.0009124·T	9.420 ±0.01	0.9999

$$\Delta G_{Ag_mIn_n}^{f} = A + BT \quad (4)$$

The lattice stabilities of pure elements were taken from Ref. 24.

Description of Surface Tension

The expression for the surface tension of the Ag-In binary liquid alloy on the basis of the Butler's model[19] is described as follows:

$$\begin{aligned}\sigma &= \sigma_{Ag} + \frac{RT}{A_{Ag}} \ln \frac{(1-x_{In}^{S})}{(1-x_{In}^{B})} + \frac{1}{A_{Ag}} \overline{G}_{Ag}^{E,S}(T, x_{In}^{S}) \\ &\quad - \frac{1}{A_{Ag}} \overline{G}_{In}^{E,B}(T, x_{In}^{B}) \\ &= \sigma_{In} + \frac{RT}{A_{Ag}} \ln \frac{x_{In}^{S}}{x_{In}^{B}} + \frac{1}{A_{In}} \overline{G}_{In}^{E,S}(T, x_{In}^{S}) \\ &\quad - \frac{1}{A_{In}} \overline{G}_{In}^{E,B}(T, x_{In}^{B})\end{aligned} \quad (5)$$

where R is the gas constant, T is absolute temperature, σ_i is the surface tension of a liquid phase of pure element i, and A_i is the molar surface area in a monolayer of liquid i (i =Ag, In). x_{In}^{S} and x_{In}^{B} are the atomic fractions in the surface and bulk, respectively. A_i can be obtained from

$$A_i = L \cdot N_0^{1/3} \cdot V_i^{2/3} \quad (6)$$

where N_0 is Avogadro's number and V_i is the molar volume of liquid i. L is usually set to be 1.091 for liquid metals assuming the close package structure of mono-

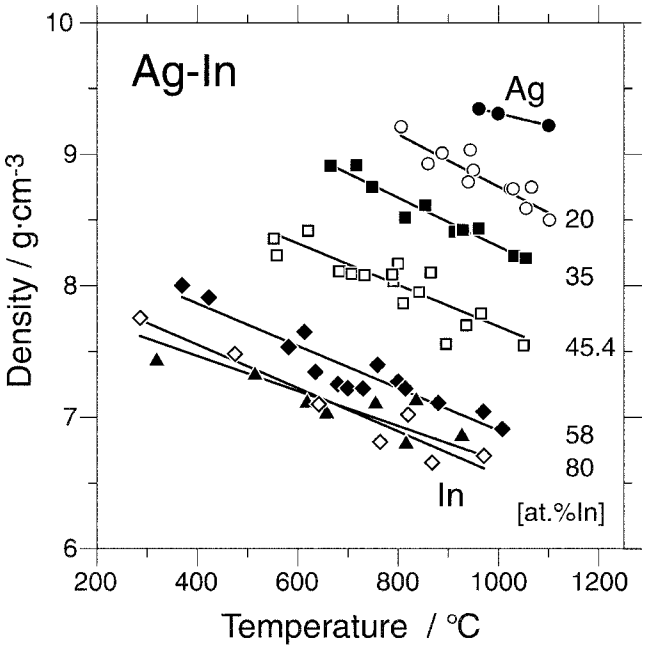

Fig. 13. Temperature dependence of the densities of the liquid Ag-In alloys. Symbols: experimental data of this study. Solid lines: average from linear equations.

layer. $\overline{G}_i^{E,S}(T, x_{In}^S)$ and $\overline{G}_i^{E,B}(T, x_{In}^B)$ represent the partial excess Gibbs energy of element i in the surface and bulk phases, respectively. Following relationship between the partial excess Gibbs energies in the bulk and surface phases was proposed:

$$\overline{G}_i^{E,S}(T, x_j^S) = \beta \cdot \overline{G}_i^{E,B}(T, x_j^B) \quad (7)$$

where β is a parameter corresponding to the ratio of the coordination number in the surface phase to that in the bulk phase, and was estimated to be β = 0.83 for liquid metals by Tanaka et al.[25]

The method for calculating the surface tension of liquid alloys proposed by Tanaka et al.[25] is used in the present calculation. The excess partial Gibbs energy $\overline{G}_i^{E,B}(T, x_j^B)$ can be obtained from the optimized thermodynamic parameters.

RESULTS AND DISCUSSION

Phase Diagram

A typical example of the microstructure and concentration profile of the Ag-15at.%In / In diffusion couple annealed at 250°C for 216 hours is shown in Fig. 2, in which four phase boundaries of the (Ag)/ ζ / Ag_2In / ζ / liquid layer structure can be clearly observed. The phase equilibrium compositions can be obtained by extrapolating the curves of the concentration profiles to the interface boundaries. Figure 3 shows the two-phase microstructure of the liquid and ζ of the Ag-50at.% In alloy annealed at 300°C for 48 hours. DSC heating curve of the Ag-22.5at.% In alloy is presented in Fig. 4. DSC results show that there are two invariant reactions at 671°C and 694°C, which may correspond to the L + (Ag) ↔ β and β + (Ag) ↔ ζ reactions, respectively, reported in previous works. These results support the existence of a β (bcc) phase with small solubility. The experimental results obtained in the present work are summarized in Tables I and II. The experimental data from the diffusion couple are in good agreement with those from two-phase alloys and DSC. By comparing the phase diagram reported in the previous works, the liquidus lines are basically in agreement with each other. However, a main difference is that the region of the ζ phase is narrower than that reported before.

The evaluation of thermodynamic parameters has been made using the computer software PARROT developed by Sundman et al.[26] The parameter of the liquid phase was optimized first using the activity and enthalpy of mixing reported in the previous investigations,[6,9–11,15,16] and then the parameter of the fcc phase was fitted based on the activity, enthalpy of mixing, and Gibbs energies reported in the previous works,[6,12–14] as well as the data for the phase boundaries between the liquid and fcc phases. Thermodynamic parameters of other phases were evaluated by taking account of the phase equilibria determined by the present work. All the optimized parameters are listed in Table III. Figure 5 shows the calculated phase diagram compared with the experimental data.[2, 5, 27-29] The calculated invariant reactions are compared with the experimental data, as listed in Table IV. The comparisons of the thermodynamic properties of enthalpy of mixing in the solid phases, chemical potential of In in the fcc phase, both the experimental and calculated results on the activity of In and the enthalpy of mixing in the liquid phase are

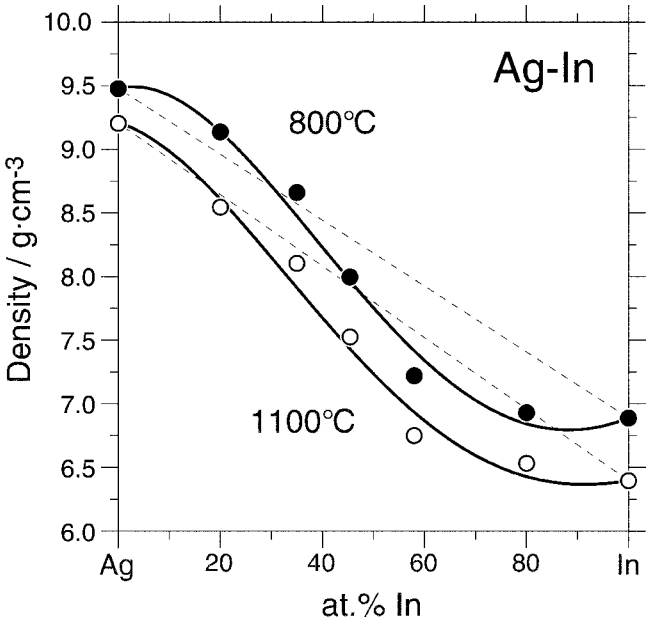

Fig. 14. Isotherms of the density of the Ag-In liquid alloys calculated at 800°C and 1100°C. Thick lines show the polynomial description of the values of the density (symbols) calculated from equations in Table VI and thin dashed lines present linear changes.

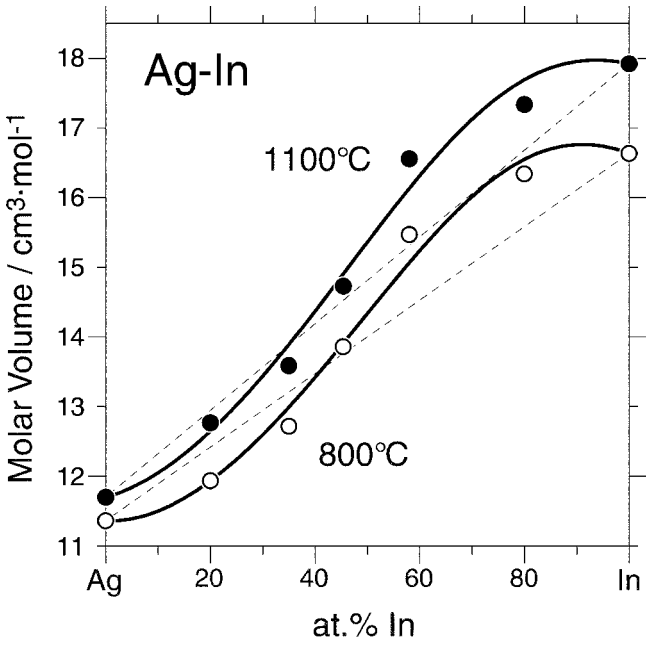

Fig. 15. Isotherms of the molar volume of the Ag-In liquid alloys calculated at 800°C and 1100°C. Symbols show the values calculated based on the density equation gathered in Table VI, thick lines show values calculated from polynomial description of the density, and thin dashed lines present the molar volume of ideal solutions.

shown in Figs. 6 to 9, respectively. It is seen that fair agreement is obtained for not only phase equilibria but also thermodynamic properties.

Surface Tension and Density

The results obtained for the surface tensions of In and Ag are presented in Figs. 10 and 11, and compared with the data from the literature.[30–43] The results of the Ag-In alloys examined are shown in Fig. 12. Application of least squares fit to the values obtained for the surface tensions is presented in Table V with standards errors for values calculated at 900°C. The results show that addition of In reduces the surface tension of pure Ag facilitating wetting.

Data obtained for densities were averaged by the least squares method and presented in Table VI with errors at 900°C. The temperature dependence of densities is presented in Fig. 13 and the isotherms of the density and the molar volume of the Ag-In liquid alloys are shown in Figs. 14 and 15.

On the basis of the excess Gibbs energy $G_i^E(T,x_j^B)$ obtained from the above assessed thermodynamic parameters, the surface tension of the liquid phase was calculated from Eq. 5.

A comparison of the calculated and experimental results for the surface tension is shown in Figs. 16 and 17. Differences of about 50 mN/m are observed for the Ag-20at.% In alloy in the temperature range from about 750°C to 1025°C, while they are equal to about 7% for the measured values. For the other alloys an agreement is much better and generally lower than 3%. The same conclusion can be derived, analyzing the isotherms shown in Fig. 17.

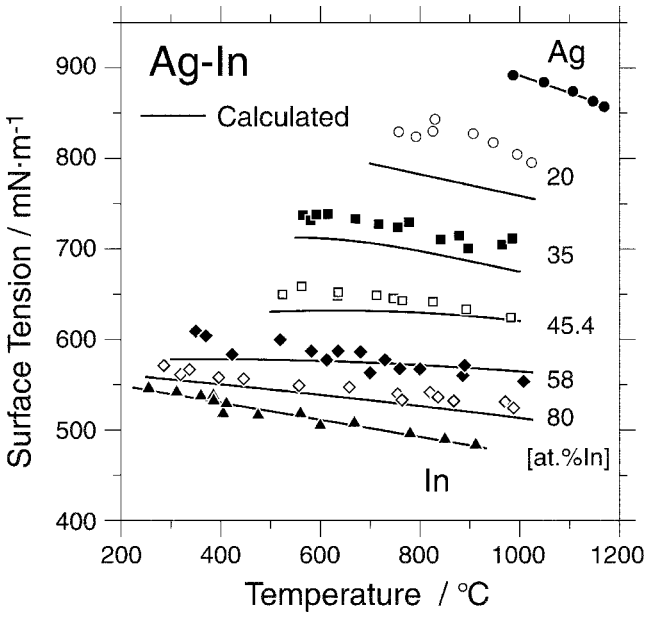

Fig. 16. Temperature dependence of the surface tension of the liquid Ag-In alloys. Symbols: experimental data of this study. Solid lines: Calculated results by Butler's method from optimized thermodynamic parameters with β = 0.83.

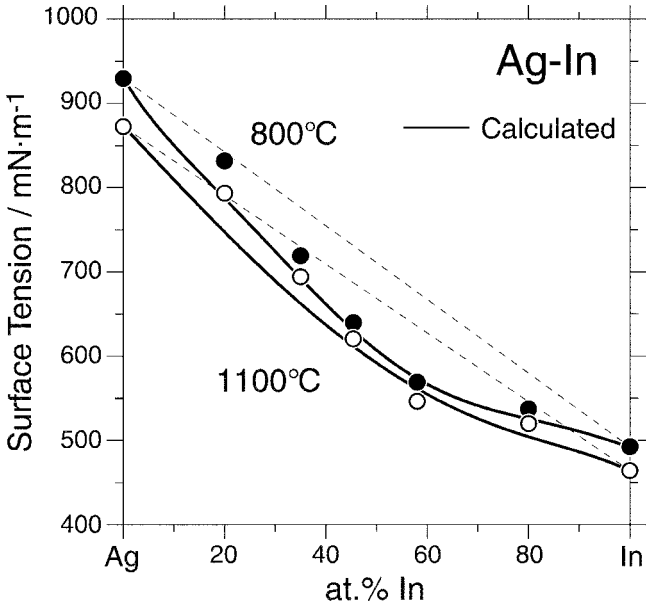

Fig. 17. Isotherms of the liquid Ag-In alloys at 800°C and 1100°C. Symbols: experimental data of this study. Solid lines: calculated results by Butler's method from optimized thermodynamic parameters with β = 0.83.

CONCLUSIONS

The phase diagram in the Ag-In system was experimentally determined by EPMA and DSC measurements. The results show that the region of ζ phase is narrower than that reported before. A thermodynamic assessment of this system is also presented based on the experimental data including thermodynamic properties and phase equilibria.

The surface tensions and densities of the liquid phase in the Ag-In system were measured using the maximum bubble pressure method, and the calculation of the surface tension of the liquid phase was performed on the basis of Butler's model. A reasonable agreement between the calculated and experimental results was obtained.

ACKNOWLEDGEMENT

One of the authors (K.I.) wishes to thank the support from The Mitsubishi Foundation.

REFERENCES

1. M.R. Baren, *Indium Alloys and their Engineering Applications*, ed. C.E.T. White and H. Okamoto (Materials Park, OH: ASM Intl.. 1993), p. 15.
2. F. Weibke, *A. Anorg. Chem.* 222, 145 (1935).
3. E. Hellner, *Z. Metallkd.* 42, 17 (1951).
4. L.L. Frevel and E. Ott, *J. Am. Chem. Soc.* 57, 228 (1935).
5. A.N. Campbell, *Can. J. Chem.* 48, 1703 (1970).
6. O.J. Kleppa, *J. Phys. Chem.* 60, 846 (1956).
7. L.R. Orr and R. Hultgren, *J. Phys. Chem.* 65, 378 (1961).
8. T. Nozaki, *Mater. Trans. JIM* 7, 52 (1966).
9. R. Beja, *C.R. Acad. Sci.* 267C, 123 (1968).
10. C.B. Alcock, *Acta Metall.* 17, 839 (1969).
11. R. Castanet, *J. Chim. Phys.* 67, 789 (1970).
12. B. Predel and U. Schallner, *Z. Metallkd*. 63, 341 (1972).
13. D.B. Masson, *Metall. Trans. A* 4A, 991 (1973).
14. C.B. Alcock, *Acta Metall*. 21, 1003 (1973).

15. K. Kameda, *J. Japan Inst. Metals* 45, 614 (1981).
16. G. Qi, *Mater. Trans. JIM* 30, 75 (1989).
17. M. Bienzle and F. Sommer, *Z. Metallkd*. 85, 766 (1994).
18. T.M. Kornenhen and J.K. Kivilahti, *J. Electron. Mater*. 27, 149 (1998).
19. J.A.V. Butler, *Proc. Roy. Soc*. 135A, 348 (1932).
20. H. Enoki, K. Ishida, and T. Nishizawa, *J. Less-Common Met*. 160, 153 (1990).
21. S. Sugden, *J. Chem. Soc*. 124, 27 (1924).
22. F. Bashforth and J.C. Adams, *An Attempt to Test the Theory of Capillary Action* (Cambridge, U.K.: Cambridge Univ. Press, 1883).
23. O. Redlich and A.T. Kister, *Ind. Eng. Chem*. 24, 345 (1948).
24. A.T. Dinsdale, *CALPHAD* 15, 317 (1991).
25. T. Tanaka, K. Hack, T. Iida, and S. Hara, *Z. Metallkd*. 87, 380 (1996).
26. B. Sundman, B. Jansson, and J.O. Andersson, *CALPHAD* 9, 153 (1985).
27. W. Huma-Rothery, *Phil. Trans. Royal Soc. London, Ser. A* 233, 1 (1936).
28. E.A. Owen, *Phil. Mag*. 27, 294 (1939).
29. M.E. Staumanis, *Trans. Metall. Soc. London AIME* 233, 964 (1965).
30. E.E. Libman, *Bull. Ill. Univ. Eng. Exp. Sta*. 187 (1928).
31. W.D. Kingery and M. Humenik, *J. Phys. Chem*. 57, 358 (1953).
32. I. Lauerman, G. Metzger, and F. Sauerwald, *Z. Phys. Chem*. Bol 216, 1 (1960).
33. S.K. Rhee, *J. Am. Ceram. Soc*. 53, 639 (1970).
34. G. Bernard and C.H.P. Lupis, *Metall. Trans*. 2, 555 (1971).
35. A. Kasama, T. Iida, and Z. Morita, *J. Jpn. Inst. Met*. 40, 1030 (1976).
36. M. Brunet, J.C. Joud, N. Eustathopoulos, and P. Desre, *J. Less Common Met*. 51, 59 (1977).
37. R. Sengiorgi, M.L. Muolo, and A. Passerone, *Acta Metall*. 30, 1597 (1982).
38. K. Nogi, K. Oishi, and K. Ogino, *Mater. Trans. JIM* 30, 137 (1989).
39. I. Egry, G. Lohófer, and S. Schneider, Paper presented at the 10th Int. IUPAC Conf. High Temperature Materials Chemistry (Julich, Germany, 10–14 April 2000), p. 87.
40. D.A. Melford and T.P. Hoar, *J. Inst. Met*. 85, 197 (1956–57).
41. S.P. Yatsenko, W.I. Kononenko, and A.L. Schukman, *Teplofiz. Vys. Temp*. 10, 66 (1972).
42. G. Lang, *J. Inst. Met*. 101, 300 (1973).
43. G. Lang, P. Laty, J.C. Joud, and P. Desre, *Z. Metallkd*. 68, 133 (1977).